Interference lithography for metal nanopattern fabrication assisted by surface plasmon polaritons reflecting image

Jingquan Wang and Huimin Liang

Articles you may be interested in

An effective medium study of surface plasmon polaritons in nanostructured gratings using attenuated total reflection
J. Appl. Phys. **115**, 013104 (2014); 10.1063/1.4856255

Surface plasmon assisted contact scheme nanoscale photolithography using an UV lamp
J. Vac. Sci. Technol. B **26**, 227 (2008); 10.1116/1.2834688

Nanopattern transfer to Si O 2 by ion track lithography and highly selective HF vapor etching
J. Vac. Sci. Technol. B **25**, 862 (2007); 10.1116/1.2738481

Field enhancement by surface plasmon polariton in self-assembling nanopatterned media
Appl. Phys. Lett. **88**, 123113 (2006); 10.1063/1.2190708

Surface-plasmon-assisted nanoscale photolithography by polarized light
Appl. Phys. Lett. **86**, 253107 (2005); 10.1063/1.1951052

Interference lithography for metal nanopattern fabrication assisted by surface plasmon polaritons reflecting image

Jingquan Wang[a)] and Huimin Liang
College of Science, Hebei University of Engineering, Handan 056038, People's Republic of China

An interference lithography technique by surface-polasmon-polaritons reflecting image is suggested for fabricating large-area metal nanopatterns in this paper. This device is designed by an attenuated total reflection mode. Enhanced interference light field is formed in the resist layer coated on any thickness metal film, which will provide a nanomask on the metal film after development. If the chemical or physical etch methods are employed, the nanomask pattern can be transferred into the metal film. Calculated and analyzed results illuminate that the incident angle, the polymer interlayer thickness, and the resist layer thickness can provide large tolerances in fabrication. © 2013 AIP Publishing LLC. [http://dx.doi.org/10.1063/1.4811530]

I. INTRODUCTION

Metal nanopatterns have been widely applied in biochemical sensors and surface optics, and its fabrication is interesting to us. However, it is important to form a nanomask on a metal film for achieving a metal nanopattern. Generally, immersion lithography,[1–4] extreme or deep ultraviolet light (EUV, DUV) lithography,[3–5] soft X-ray lithography,[6] and electronic beam lithography[7,8] are employed to fabricate nanomasks on a metal film. The metal nanopatterns can be achieved by using chemical or physical etch methods. However, the effective wavelength in the immersion lithography will depend on the liquid refractivity, and suitable liquid materials are very few. Although EUV, DUV, soft X-ray, and electronic beam lithography can fabricate high-quality nanomasks, they are still very costly and complex. Presently, interference lithography techniques assisted by surface-plasmon-polaritions (SPP) can generate nanopatterns easily beyond the diffraction limit,[9–20] but these techniques cannot form an interference pattern on any thickness metal film.

In this paper, we suggest a lithography technique assisted by SPP reflecting image (SPPRI) for fabricating periodic metal nanopatterns with any thickness, and we call this technique SPPRI lithography (SPPRIL). This device is designed based on an attenuated total reflection (ATR) mode. The metal film thickness does not influence the intensity of SPP interference pattern in this scheme, which can provide a high-quality and stable nanomask on the metal film after exposure and development. Another advantage of this SPPRIL is that this design can generate easily tight contact between the resist coated on a metal film and the polymer coated under a prism by an appropriate outside force since they all are soft materials. Besides, the tolerances of the polymer thickness, the resist thickness, and the incident angle have been calculated and analyzed in detail for experiment.

II. SPPRIL SCHEME AND INTERFERENCE-FIELD DISTRIBUTION

The schematic configuration is shown in Fig. 1. The polymer layer is coated under the prism. The metal film is coated on the substrate, and the resist layer is recoated on the metal film. The refractive indices of prism, polymer, resist, metal film and substrate are n_0, n_1, n_2, n_3, and n_4, respectively. θ is the incident angle. The thicknesses of the polymer, resist and metal film are d_p, d_r, and d_m, respectively. When two TM waves with the resonance angle irradiate the interface of the prism and polymer symmetrically, enhanced SPP interference will be excited on the metal film. After exposure and developing, a nanomask is formed on the metal film. The nanomask can be transferred into the metal film if we further employ chemical or physical method to etch the metal film. Moreover, this design can conquer the influence of the air gap between the polymer and the resist to a certain extent since they are soft materials.

When one TM plane wave transmits into this multilayer structure, the light-field distribution in each layer can be written as

$$\begin{cases} H_{ly} = (a_l e^{ik_{lx}x} + b_l e^{-ik_{lx}x})e^{ik_z z} \\ E_{lx} = \dfrac{k_z}{\omega\varepsilon_l}(a_l e^{ik_{lx}x} + b_l e^{-ik_{lx}x})e^{ik_z z} \\ E_{lz} = -\dfrac{k_{lx}}{\omega\varepsilon_l}(a_l e^{ik_{lx}x} - b_l e^{-ik_{lx}x})e^{ik_z z} \end{cases} \quad (l = 0, 1, \dots) \quad (1)$$
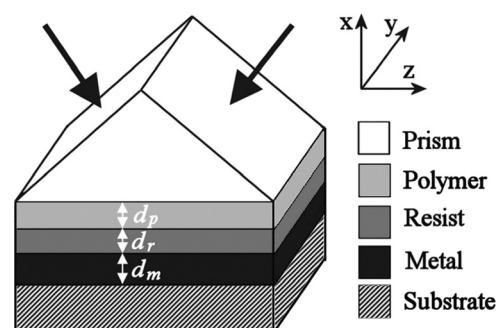

FIG. 1. The schematic configuration of SPPRIL, and composed of prism, polymer, resist, metal, and substrate.

a)Author to whom correspondence should be addressed. Electronic mail: jingquanwang1212@163.com.

113, 233101-1

and

$$\begin{cases} k_{lx} = \dfrac{\omega}{c}\sqrt{\varepsilon_l - \varepsilon_0 \sin^2\theta} \\ k_z = \dfrac{\omega}{c}\sqrt{\varepsilon_0}\sin\theta \qquad (l = 0,\,1,\,\ldots), \\ \varepsilon_l = n_l^2 \end{cases} \qquad (2)$$

where a_l and b_l are the transmission coefficients along $+x$ and $-x$ directions in each layer, respectively.

The continuous conditions at each interface can be expressed as

$$\begin{cases} H_{ly} = H_{(l+1)y} \\ E_{lz} = E_{(l+1)z}. \end{cases} \qquad (3)$$

The coefficients of a_l and b_l can be solved by formula (1)–(3). So the total reflectivity in SPPRIL system can be expressed as

$$R_0 = |a_0|^2. \qquad (4)$$

In our investigation, the metal permittivity is given by Lorentz-Drude (LD) oscillator model,[21]

$$\varepsilon_r(\omega) = \varepsilon_r^f(\omega) + \varepsilon_r^b(\omega), \qquad (5)$$

where $\varepsilon_r^f(\omega)$ and $\varepsilon_r^b(\omega)$ are the Drude model and the Lorentz model, respectively.

In SPPRIL, the evolution of the total reflectivity (R_0) is calculated with the incident angle (θ) and the resist thickness (d_r) when the polymer thickness (d_p) and the metal film thickness (d_m) are constant, and the result is shown in Fig. 2. In this calculation, d_p and d_m are 0.1 μm and 0.1 μm, respectively. The refractive indices of n_0, n_1, n_2, and n_4 are 2.14 (K-PSFn214), $1.6 + 0.003i$, $1.61 + 0.003i$, and 1.47, respectively. The metal is aluminum (Al), and its permittivity (ε_3) is $-26.75+5.85i$ at the illuminating wavelength of 441 nm calculated by Eq. (5). When $d_r = 0.085$ μm and $\theta = 51.9°$, $R_0 = 0$, which means that SPP intensity reaches a maximum value.

The light-field distribution from prism to substrate vertically at $R_0 = 0$ is shown in Fig. 3. Due to SPP resonance with the incident light, the intensity of the evanescent wave in the
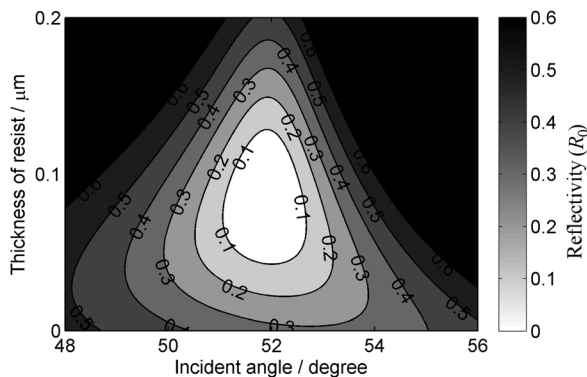

FIG. 3. Intensity distribution in SPPRIL at one TM or TE plane wave irradiating with $d_p = 0.1$ μm, $d_r = 0.085$ μm, $d_m = 0.1$ μm and $\theta = 51.9°$.

resist layer is enhanced dramatically. The intensity ($|H_y|^2/|H_0|^2$) is increased about 10 times at the interface of the resist and the metal (n_2/n_3), and about 3 times at the interface of the polymer and the resist (n_1/n_2). But if the incident light is TE wave, the intensity ($|E_y|^2/|E_0|^2$) is extremely weak in the resist layer since without SPP resonance. That is, it is very difficult to generate a nanomask on the metal film using the interference of TE waves exciting evanescent waves.

The interference result of two TM waves launching SPP is generated on the metal film and shown in Fig. 4. Fig. 4(a) depicts the light-field distribution of the resist on the metal film, and Fig. 4(b) is the distribution of cross section at y = 0. Since $R_0 = 0$, the incident energy transfers into SPP wave completely, and the intensity of the interference fringes on the metal film is enhanced obviously. The period of the interference pattern is 131 nm, and if the half peak width takes as the feature size, the critical dimension is 66 nm. As SPP attenuates exponentially along $+x$ direction, the intensity of the interference fringes at n_2/n_3 is far more than that at n_1/n_2, which means that the exposure dose of the bottom resist is more than that of the top resist, and reaches a maximum at the interface of n_2/n_3. However, this exposure distribution is useful to form a nanomask similar to a binary grating on the metal film. The reason is that the developer concentration will decrease with the increase of the resist

FIG. 2. Reflectivity varying with incident angle and resist thickness in SPPRIL, $d_p = 0.1 \mu$m and $d_m = 0.1 \mu$m are constant.
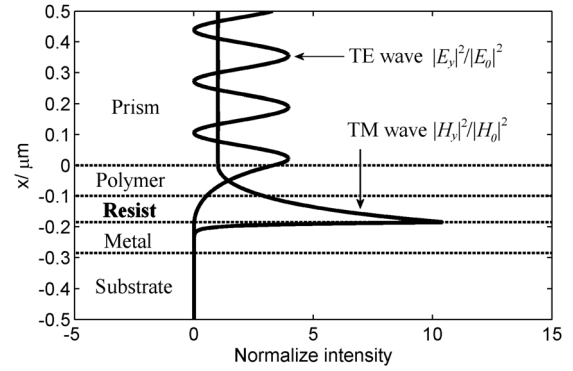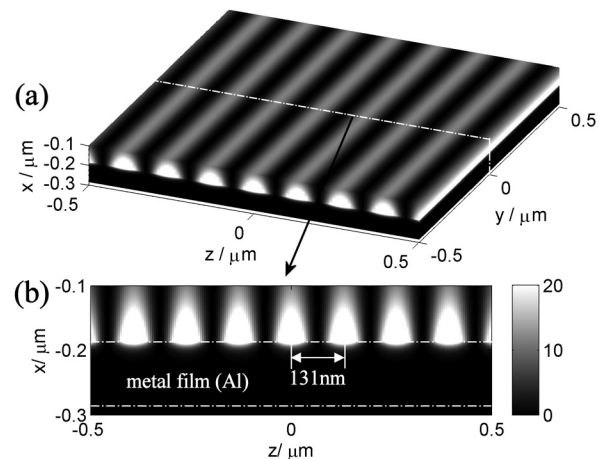

FIG. 4. Two SPP interference result on the metal film, (a) light field distribution in the resist and the metal film, (b) the intensity distributions of cross section at y = 0.
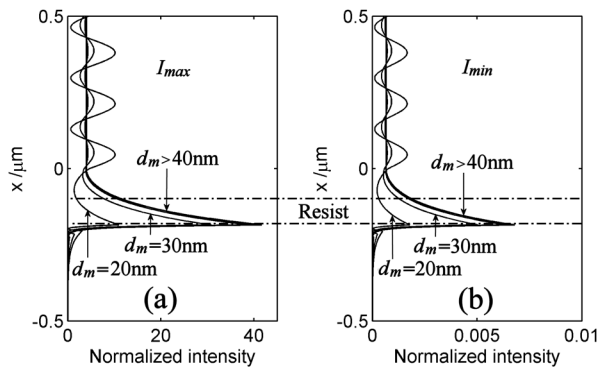
FIG. 5. Vertical intensity distribution of one interference fringe varying with different metal film thicknesses, (a) the maximum intensity (I_{max}) and (b) minimum intensity (I_{min}).

FIG. 7. Variation of the intensity at polymer/resist (n_1/n_2) and resist/metal (n_2/n_3) with different (a) polymer thickness d_p ($d_m = 0.1 \mu m$, $d_r = 0.085 \mu m$, and $\theta = 51.9°$), (b) resist thickness d_r ($d_p = 0.1 \mu m$, $d_m = 0.1 \mu m$, and $\theta = 51.9°$) and (c) incident angle θ ($d_p = 0.1 \mu m$, $d_r = 0.085 \mu m$, and $d_m = 0.1 \mu m$).

depth in the developing process, and exposure and development can compensate each other.

The intensity evolution of interference fringes with different metal film thickness (d_m) is shown in Fig. 5. In this calculation, other parameters are constant except d_m. Figs. 5(a) and 5(b) depict the maximum and the minimum intensity (I_{max} and I_{min}) distributions of one interference fringe at x direction, respectively. In the range of $d_m < 40$ nm, the variation of the intensity distribution in the resist is acute. But when $d_m > 40$ nm, the intensity distribution in the resist reaches a stable state. In our opinion, $d_m > 30$ nm is feasible to enhance the intensity of interference pattern in SPPRIL. Furthermore, comparing two figures, I_{max} is far more than I_{min}, which proves that the interference pattern has an excellent contrast.

If the incident beams are more than two beams, interference patterns of dot array can be formed on the metal film, as shown in Fig. 6. In this calculation, $d_r = 0.085 \mu m$ and $d_m = 0.1 \mu m$. Figs. 6(a) and 6(b) depict the interference patterns when four and six beams launch SPP symmetrically,

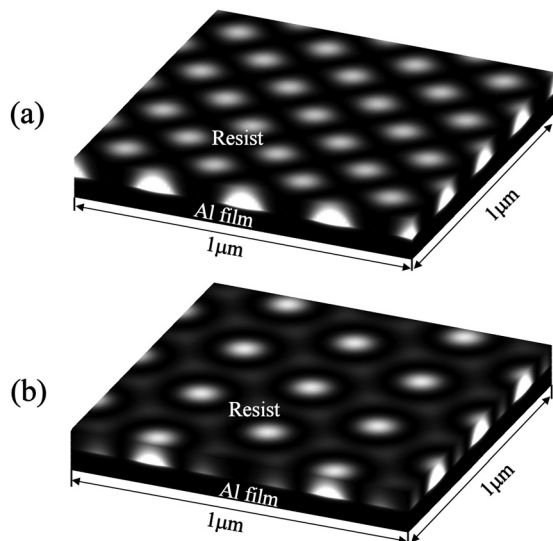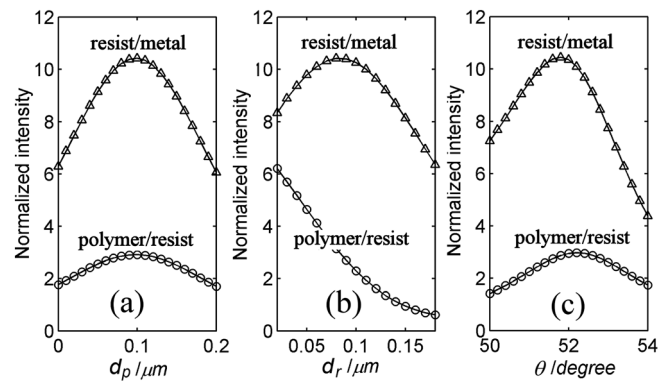respectively. This means that we also can fabricate the metal pattern of nano-dot array.

III. TOLERANCE DISCUSSION

It is necessary to discuss the intensity variation with different d_p, d_r, and θ for experiment. Fig. 7 shows the intensity evolution of two interfaces connecting the resist (n_1/n_2 and n_2/n_3) with these parameters. In each parameter discussion, we set other parameters as constants. Since the intensity decreases exponentially along $+x$ direction in SPPRIL, the intensity at the upper surface of the resist is a key. If we take $|H_y|^2/|H_0|^2 = 2$ as a threshold to estimate the tolerances of these parameters, the tolerance ranges of d_p, d_r and θ can be given by Figs. 7(a)–7(c), and they are $0.02 \mu m$ to $0.18 \mu m$ at $d_m = 0.1 \mu m$, $d_r = 0.085 \mu m$ and $\theta = 51.9°$, less than $0.11 \mu m$ at $d_p = 0.1 \mu m$, $d_m = 0.1 \mu m$ and $\theta = 51.9°$ and 50.8 to $53.6°$ at $d_p = 0.1 \mu m$, $d_r = 0.085 \mu m$ and $d_m = 0.1 \mu m$, respectively. Especially, Fig. 7(c) also represents a resolution modulation from 133 nm to 128 nm. Apparently, the small range ($\sim$5 nm) for the resolution is not enough to the application. In order to enlarge the resolution range of this lithography, we can modulate the exposure time to a certain extent in experiment.

IV. CONCLUSION

In conclusion, an SPPRIL technique for fabricating periodic metal nanopatterns has been demonstrated in this paper. Calculated and analyzed results indicate that enhanced interference nanopatterns can be achieved easily on a metal film by this scheme, and the intensity of the inference fringes is not varied evidently with different metal film thickness, which means that we can fabricate nanomasks on any thickness metal film by this SPPRIL. When we employ chemical or physical methods to etch the metal film, the nanopattern will be transferred into the metal film. The incident angle and the thicknesses of the polymer and the resist in the model have been analyzed in details, and they all can provide large tolerances for experiment. Moreover, since the polymer under the prism and the resist on the metal film are all soft material in the design, the air gap influence will be reduce largely for experiment.

FIG. 6. Evolution of SPP interference patterns on the metal film with different incident beams, (a) four beams, and (b) six beams.

ACKNOWLEDGMENTS

[1]C. A. Mack, Proc. SPIE **5374**, 1–8 (2004).

[2]F. M. Schellenberg, Proc. SPIE **5377**, 1–20 (2004).

[3]M. Switkes and M. Rothschild, J. Vac. Sci. Technol. B **19**, 2353–2356 (2001).

[4]J. A. Hoffnagle, W. D. Hinsberg, M. Sanchez, and F. A. Houle, J. Vac. Sci. Technol. B **17**, 3306–3309 (1999).

[5]C. W. Gwyn, R. Stulen, D. Sweeney, and D. Attwood, J. Vac. Sci. Technol. B **16**, 3142–3149 (1998).

[6]J. P. Silverman, J. Vac. Sci. Technol. B **16**, 3137–3141 (1998).

[7]E. H. Anderson, IEEE J. Quantum Electron. **42**, 27–35 (2006).

[8]J. Fujita, Y. Ohnishi, Y. Ochiai, and S. Matsui, Appl. Phys. Lett. **68**, 1297–1299 (1996).

[9]X. W. Guo, J. L. Du, Y. K. Guo, and J. Yao, Opt. Lett. **31**, 2613–2615 (2006).

[10]E. A. Bezus, D. A. Bykov, L. L. Doskolovich, and I. I. Kadomin, J. Opt. A: Pure Appl. Opt. **10**, 095204 (2008).

[11]X. W. Guo, J. L. Du, X. G. Luo, C. L. Du, and Y. K. Guo, Microelectron. Eng. **84**, 1037–1040 (2007).

[12]A. Bouhelier, H. Ignatovich, A. Bruyant, C. Huang, G. C. Francs, J. C. Weeber, A. Dereux, G. P. Wiederrecht, and L. Novotny, Opt. Lett. **32**, 2535–2537 (2007).

[13]Y. Lim, S. Kim, H. Kim, J. Jung, and B. Lee, IEEE J. Quantum Electron. **44**, 305–311 (2008).

[14]V. M. Murukeshan and K. V. Sreekanth, Opt. Lett. **34**, 845–847 (2009).

[15]K. V. Sreekanth and V. M. Murukeshan, J. Vac. Sci. Technol. B **28**, 128–130 (2010).

[16]X. Luo and T. Ishihara, Appl. Phys. Lett. **84**, 4780–4782 (2004).

[17]W. Srituravanich, N. Fang, S. Durant, M. Ambati, C. Sun, and X. Zhang, J. Vac. Sci. Technol. B **22**, 3475–3478 (2004).

[18]Z. Liu, Q. Wei, and X. Zhang, Nano Lett. **5**, 957–961 (2005).

[19]B. Zeng, L. Pan, L. Liu, L. Fang, C. Wang, and X. Luo, J. Opt. A: Pure Appl. Opt. **11**, 125003 (2009).

[20]X. Guo and Q. Dong, J. Appl. Phys. **108**, 113108 (2010).

[21]A. D. Rakic, A. B. Djurisic, J. M. Elazar, and M. L. Majewski, Appl. Opt. **37**, 5271–5283 (1998).